“© 2021 IEEE. Personal use of this material is permitted. Permission from IEEE must be obtained for all other uses, in any current or future media, including reprinting/republishing this material for advertising or promotional purposes, creating new collective works, for resale or redistribution to servers or lists, or reuse of any copyrighted component of this work in other works.”

Nullification of Multiple Correlated Jammers

Linh Hoang*, J. Andrew Zhang*, Diep Nguyen*,
Asanka Kekirigoda† and Kin-Ping Hui†
* Global Big Data Technologies Centre, University of Technology Sydney, Sydney, Australia
† Defence Science and Technology (DST), Edinburgh, Australia
Emails: {Linh.M.Hoang}@student.uts.edu.au; {Andrew.Zhang; Diep.Nguyen}@uts.edu.au;
{Asanka.Kekirigoda; Kinping.Hui}@dst.defence.gov.au

***Abstract*—Effective suppression of the intentional jamming signals is crucial to ensure reliable wireless communication. However, as demonstrated in this paper, when the transmitted jamming signals are highly correlated, and especially when the correlations between transmitted jamming signals are deliberately varied over time, nullifying the jamming signals can be challenging. Unlike existing studies assuming uncorrelated jamming signals or non-zero but constant correlations, we evaluate the impact of the non-zero and varying correlations on the suppression of the jamming signals. We discover that by varying the correlations between transmitted jamming signals, jammers can "virtually change" the jamming channels hence their nullspace, even when these channels do not physically change. That makes most jamming suppression techniques that rely on steering receiving beams towards the nullspace of jamming channels no longer applicable. To tackle the problem, we develop techniques to effectively track the jamming nullspace and update the receiving beams accordingly. It is demonstrated by Monte Carlo simulations that our proposed techniques can suppress/nullify jamming signals for all considered scenarios with non-zero and varying correlations amongst jamming signals.**

***Index Terms*—jamming suppression, multi-user MIMO, correlated jamming signals**

I. Introduction

Wireless communication is susceptible to radio-frequency (RF) jamming, which either inadvertently or deliberately disrupts the signal reception/decoding. This is one of the most serious threats to reliable wireless communications. Among different jammers types, proactive jammers are the most common ones due to their simplicity [1]. In the case of malicious jammers, a smart jammer can design the jamming signals to counteract jamming suppression techniques, which makes jamming suppression even more challenging.

One conventional approach to suppress jamming is by using the angle of arrival (AOA)-based beam-forming techniques. It is realized by forming receiving beam nulls towards the estimated AOAs. However, the receiver has to "sacrifice" at least one degree-of-freedom to nullify each jamming spatial stream [2]. That makes the approach not suitable when the number of jammers is large, or when the signal from each jammer reaches the receiver through a large number of propagation paths (e.g., in the urban areas).

This research is supported by the Commonwealth of Australia as represented by the Defence Science and Technology Group of the Department of Defence.

Alternatively, jamming suppression can be realized by estimating the projection of jamming channels [3]–[5], the ratios between jamming channels [6], or the nullspace of jamming channel [7], and then designing filters to nullify the jamming signals. These methods require only one degree-of-freedom to nullify each spatial stream of an jammer, which is much more effective than the aforementioned AOA-based technique. The interference rejection combining (IRC) technique [8] considers the impact of the correlations between interference channels on interference suppression performance. However, the techniques in [3]–[8] do not consider the impact of the correlations between transmitted jamming signals on the jamming nullification performance. In [9] and [10], the authors show that, by choosing suitable correlations, the jammers can maximize the jamming impact to communications between legitimate devices. Therefore, to ensure the effectiveness of the jamming suppression techniques, it is crucial to take into consideration the correlations. Nonetheless, the objective of [9] and [10] is to analyze the impact of the correlations between transmitted jamming signals on the jamming outcome. The two papers neither propose any suppression technique for correlated jamming nor discuss the impact of the correlations on such an jamming nullification method. Another unanswered question is the impact of varying non-zero correlations coefficients between transmitted jamming signals on the jamming suppression process.

In fact, if ignoring the RF ineffectiveness in sacrificing the antennas or degree-of-freedom, the AOA-based beam-forming technique described above can deal quite well in the cases with non-zero correlations between transmitted jamming signals. Specifically, when the jamming signals are correlated, the spatial smoothing technique [11] can be applied to decorrelate the jamming signals and estimate their AOAs. However, as aforementioned, a large number of antennas are required to nullify each spatial stream of a jammer, making the AOA based beam-forming techniques inappropriate when the number of jammers is large, or the signal from each jammer arrives the receiver via multiple independent propagation paths.

This paper studies the impact of the non-zero and varying correlations between transmitted jamming signals on the jamming suppression. We prove that the effect of non-zero and varying correlations between transmitted jamming signals on the jamming suppression process is similar to that under the time-varying channels. This finding then guides us to

develop jamming nullification techniques that effectively track the jamming nullspace and correspondingly update receiving beams under all levels of varying correlations between transmitted jamming signals. Our proposed techniques cost only a single degree-of-freedom of receiving antennas to nullify each jammers' spatial stream. Monte Carlo simulations are provided, showing that our techniques are capable of suppressing the jamming signals for all considered scenarios with non-zero and varying correlations coefficients (between transmitted jamming signals).

II. Problem Formulation

We consider a multi-user multiple-input multiple-output (MU-MIMO) downlink system, where the base station (BS) communicates with K user equipment (UE). The BS and the kth UE have N_T and N_k antennas, respectively. The number of independent data streams from the BS to the kth UE is D_k. There are N_J single-antenna proactive jammers that interfere with BS-UEs communication. Note that this paper's techniques are also suitable for multiple-antennas jammers because a multiple-antennas jammer can be considered multiple single-antenna jammers.

The received signals at the kth UE is given by

$$\mathbf{y}_k = \mathbf{H}_k\mathbf{P}_k\mathbf{x}_k + \mathbf{H}_k\sum_{l\neq k}^{K}\mathbf{P}_l\mathbf{x}_l + \mathbf{Z}_k\mathbf{x}_{\mathrm{J}} + \mathbf{n}, \tag{1}$$

where $\mathbf{H}_k \in \mathbb{C}^{N_k\times N_T}$ denotes the channel between the BS and the kth UE, $\mathbf{P}_k \in \mathbb{C}^{N_T\times D_k}$ is the precoding matrix for the kth UE, $\mathbf{x}_k \in \mathbb{C}^{D_k\times 1}$ denotes the transmitted signal from the BS to the kth UE, $\mathbf{Z}_k \in \mathbb{C}^{N_k\times N_J}$ is the channel matrix between N_J jammers and the kth UE, $\mathbf{x}_{\mathrm{J}} = [x_{\mathrm{J}1}; x_{\mathrm{J}2}; ...; x_{\mathrm{J}N_J}] \in \mathbb{C}^{N_J\times 1}$ stands for the transmitted jamming signals, and $\mathbf{n} \in \mathbb{C}^{N_k\times 1}$ is complex noise. We assume that the elements of $\mathbf{n}$ are independent and identically distributed (i.i.d.) zero-mean circularly-symmetric complex Gaussian random variables (i.e., $\mathbf{n} \sim \mathcal{CN}(\mathbf{0}, \sigma_n^2\mathbf{I}_{N_k})$, where $\mathbf{I}_{N_k}$ denotes an identity matrix of size N_k). Similarly, we assume $\mathbf{x}_k \sim \mathcal{CN}(\mathbf{0}, \mathbf{\Sigma}_{\mathbf{x}_k})$ and $\mathbf{x}_{\mathrm{J}} \sim \mathcal{CN}(\mathbf{0}, \mathbf{\Sigma}_{\mathrm{J}})$, where $\mathbf{\Sigma}_{\mathbf{x}_k}$ and $\mathbf{\Sigma}_{\mathrm{J}}$ are the covariance matrices of the transmitted signal from the BS (to the kth UE) and the jammers, respectively. We assume that the jammers, if more than one, can coordinate to control $\mathbf{\Sigma}_{\mathrm{J}}$. The channels $\mathbf{H}_k$ and $\mathbf{Z}_k$ are both modeled using a flat fast fading Rician channel model from [12]. The detailed parameters are given in the Simulation section. For ease of reference, important symbols and notations are summarized in Table I. Note that we use superscripts "s", "d", and "i" to represent symbols in the (inter-frame) silent period, data transmission period, and intra-frame silent period, respectively.

In the subspace-based approach, jamming nullification is achieved by multiplying the received signal with a beam-forming matrix derived from the left nullspace [13, p. 181] of the received jamming signals. The received signal after nullification can be represented as [14],

$$\mathbf{p}_k = \mathbf{W}_k(\mathbf{H}_k\mathbf{P}_k\mathbf{x}_k + \mathbf{H}_k\sum_{l\neq k}^{K}\mathbf{P}_l\mathbf{x}_l + \mathbf{Z}_k\mathbf{x}_{\mathrm{J}} + \mathbf{n}), \tag{2}$$

where $\mathbf{W}_k$ is the beam-forming matrix used to nullify the received jamming signals.

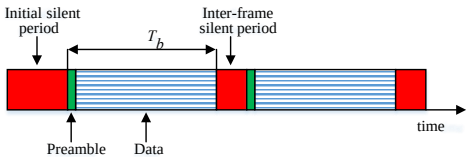

Fig. 1: Baseline protocol.

Fig. 1 represents our proposed baseline protocol based on that in [8]. It starts with a silent period, during which the BS does not send any signal, and $\mathbf{Q}_k^{\mathrm{s}} \in \mathbb{C}^{(N_k-N_J)\times N_k}$ is estimated for the first time. Note that, as summarized in Table I, $\mathbf{Q}_k^{\mathrm{s}}$ denotes the matrix whose rows form an orthonormal basis for the left nullspace of the received jamming signal at the kth UE in the inter-frame silent period. The algorithm to estimate $\mathbf{Q}_k^{\mathrm{s}}$ will be given in Subsection III-A. The estimated value of $\mathbf{Q}_k^{\mathrm{s}}$ is denoted by $\hat{\mathbf{Q}}_k^{\mathrm{s}}$. Based on $\hat{\mathbf{Q}}_k^{\mathrm{s}}$, we can design $\mathbf{W}_k$ by selecting B_k rows of $\mathbf{W}_k \in \mathbb{C}^{B_k\times N_k}$ from the $(N_k - N_J)$ rows of $\hat{\mathbf{Q}}_k^{\mathrm{s}}$. It is worth noting that B_k should be greater than or equal to D_k for successful BS-UE signal multiplexing at the receiver. Therefore, it is required that $(N_k - N_J) \geq B_k \geq D_k$ for both jamming nullification and BS-UE signal multiplexing. In this paper, we use $\mathbf{W}_k = \hat{\mathbf{Q}}_k^{\mathrm{s}}$ (i.e., by setting $B_k = N_k - N_J$), so that the receiver can exploit all of the remaining $(N_k - N_J)$ degree-of-freedoms for signal multiplexing. Because the jamming signals are mostly removed by using $\mathbf{W}_k$, the equivalent channel $\mathbf{H}_k^{\mathrm{eq}} = \mathbf{W}_k\mathbf{H}_k\mathbf{P}_k$ can be estimated by using training signals and a minimum mean-square error (MMSE) or least-square (LS) channel estimator. Equalizers such as MMSE or zero-forcing (ZF), can then be applied to find the equalization coefficients, denoted by $\mathbf{G}_k$. Then, BS-UE data transmission can be carried out. The time interval of each frame is T_b.

The effectiveness of the jamming nullification depends on how close $\hat{\mathbf{Q}}_k^{\mathrm{s}}$ is to $\mathbf{Q}_k^{\mathrm{d}}$, where $\mathbf{Q}_k^{\mathrm{d}}$ denotes the matrix whose rows form an orthonormal basis for the left nullspace of the received jamming signals at the kth UE in the data transmission period. The closer $\hat{\mathbf{Q}}_k^{\mathrm{s}}$ to $\mathbf{Q}_k^{\mathrm{d}}$ results in the better jamming nullification. The first factor that affects the similarity between $\hat{\mathbf{Q}}_k^{\mathrm{s}}$ and $\mathbf{Q}_k^{\mathrm{d}}$ is how relatively frequent $\hat{\mathbf{Q}}_k^{\mathrm{s}}$ is updated. In practice, a more frequent update of $\hat{\mathbf{Q}}_k^{\mathrm{s}}$ makes it closer to $\mathbf{Q}_k^{\mathrm{d}}$, and leads to less residual jamming after the jamming nullification process. On the other hand, the more frequent update of $\hat{\mathbf{Q}}_k^{\mathrm{s}}$ also increases the system's overhead, and less time is available for BS-UE communication. The second factor that affects the similarity between $\hat{\mathbf{Q}}_k^{\mathrm{s}}$ and $\mathbf{Q}_k^{\mathrm{d}}$, and is the focus of this paper, is the time-varying correlations between transmitted jamming signals. Due to the second factor, the jammers can intentionally vary the correlations to make jamming nullification more challenging.

While the impact of the first factor on jamming nullification performance is well investigated, the existing studies seldom consider the impact of the intentional time-varying correlations between transmitted jamming signals on the performance of jamming nullification techniques. The problems we would like to investigate are as follows.

- Characterize the impact of the time-varying correlations

TABLE I: Summary of symbols and notations.

Notation	Description
$\mathbf{x}_{\mathrm{J}}^{\mathrm{s}}$, $\mathbf{x}_{\mathrm{J}}^{\mathrm{d}}$, $\mathbf{x}_{\mathrm{J}}^{\mathrm{i}}$	Transmitted jamming signals in the inter-frame silent, data transmission, and intra-frame silent periods, respectively.
$\mathbf{\Sigma}_{\mathrm{J}}^{\mathrm{s}}$, $\mathbf{\Sigma}_{\mathrm{J}}^{\mathrm{d}}$, $\mathbf{\Sigma}_{\mathrm{J}}^{\mathrm{i}}$	Covariance matrix of $\mathbf{x}_{\mathrm{J}}^{\mathrm{s}}$, $\mathbf{x}_{\mathrm{J}}^{\mathrm{d}}$, and $\mathbf{x}_{\mathrm{J}}^{\mathrm{i}}$, respectively.
$\mathbf{y}_{\mathrm{J}_k}^{\mathrm{s}}$ $\mathbf{y}_{\mathrm{J}_k}^{\mathrm{d}}$ $\mathbf{y}_{\mathrm{J}_k}^{\mathrm{i}}$	Received jamming signals at the kth UE in the (inter-frame) silent, data transmission, and intra-frame silent periods, respectively.
$\mathbf{R}_{\mathrm{J}_k}^{\mathrm{s}}$, $\mathbf{R}_{\mathrm{J}_k}^{\mathrm{d}}$, $\mathbf{R}_{\mathrm{J}_k}^{\mathrm{i}}$	Sample covariance matrix of $\mathbf{y}_{\mathrm{J}_k}^{\mathrm{s}}$, $\mathbf{y}_{\mathrm{J}_k}^{\mathrm{d}}$, and $\mathbf{y}_{\mathrm{J}_k}^{\mathrm{i}}$, respectively.
$\mathbf{Q}_k^{\mathrm{s}}$, $\mathbf{Q}_k^{\mathrm{d}}$, $\mathbf{Q}_k^{\mathrm{i}}$	Matrix whose rows form an orthornomal basis for the left nullspace [13, p. 181] of $\mathbf{y}_{\mathrm{J}_k}^{\mathrm{s}}$, $\mathbf{y}_{\mathrm{J}_k}^{\mathrm{d}}$, and $\mathbf{y}_{\mathrm{J}_k}^{\mathrm{i}}$, respectively.
$\mathbf{Z}_k^{\mathrm{s}}$, $\mathbf{Z}_k^{\mathrm{d}}$, $\mathbf{Z}_k^{\mathrm{i}}$	Jamming channels of the kth UE in the (inter-frame) silent, data transmission, and intra-frame silent periods, respectively.
$\mathbf{W}_k$	Beam-forming matrix for the kth UE.
$\lvert.\rvert$, $\lvert\lvert.\rvert\rvert$	Complex number's modulus and matrix' Frobenius norm, respectively.
$(.)^T$, $(.)^*$, $(.)^H$, $(.)^{-1}$	Matrix's transpose, conjugate, conjugate (Hermitian) transpose, inverse, respectively.
T_c, T_b, T_ρ	Channel's coherence time, time interval of each frame, and correlations' coherence time, respectively.

between transmitted jamming signals on jamming nullification.

- Design jamming nullification techniques for different scenarios of the correlations between transmitted jamming signals.

III. Impact of the Correlation between Transmitted Interference Signals

This section demonstrates that the time-varying correlations between transmitted jamming signals causes a "virtual change" in $\mathbf{Z}_k$. Therefore, even though $\mathbf{Z}_k$ is constant, using $\hat{\mathbf{Q}}_k^{\mathrm{s}}$ to generate $\mathbf{W}_k$ may not guarantee jamming nullification. Note that, in this section, to emphasize the impact of the time-varying correlations but not the time-varying physical channel on jamming nullification, we assume that the jamming channel is under a slow block fading with coherence time $T_c \gg T_b$. Therefore, the jamming channel is considered unchanged over each frame, such that $\mathbf{Z}_k^{\mathrm{s}} = \mathbf{Z}_k^{\mathrm{d}} = \mathbf{Z}_k$. For brevity, in this section, we only use $\mathbf{Z}_k$ to represent the jamming channel.

A. Algorithm for Estimating $\mathbf{Q}_k^{\mathrm{s}}$

As mentioned in Section II, $\mathbf{Q}_k^{\mathrm{s}}$ is estimated in the inter-frame silent periods, during which the BS does not send any signal. Let $\mathbf{y}_{\mathrm{J}_k}^{\mathrm{s}}$ denotes the received jamming signal at the kth UE in the inter-frame silent period, from (1),

$$\mathbf{y}_{\mathrm{J}_k}^{\mathrm{s}} = \mathbf{Z}_k \mathbf{x}_{\mathrm{J}}^{\mathrm{s}} + \mathbf{n}, \tag{3}$$

where $\mathbf{x}_{\mathrm{J}}^{\mathrm{s}}$ is the transmitted jamming signals in the inter-frame silent period. Let

$$\mathbf{R}_{\mathrm{J}_k}^{\mathrm{s}} = \frac{1}{N_{\mathrm{s}}} \mathbf{Y}_{\mathrm{J}_k}^{\mathrm{s}} (\mathbf{Y}_{\mathrm{J}_k}^{\mathrm{s}})^H \tag{4}$$

be a sample covariance matrix of $\mathbf{y}_{\mathrm{J}_k}^{\mathrm{s}}$, where $\mathbf{Y}_{\mathrm{J}_k}^{\mathrm{s}}$ is a set containing N_{s} samples of $\mathbf{y}_{\mathrm{J}_k}^{\mathrm{s}}$. We obtain $\hat{\mathbf{Q}}_k^{\mathrm{s}}$ by

$$\hat{\mathbf{Q}}_k^{\mathrm{s}} = (\mathbf{U}_{\mathrm{n}}^{\mathrm{s}})^H, \tag{5}$$

where $\mathbf{U}_{\mathrm{n}}^{\mathrm{s}} \in \mathbb{C}^{N_k \times (N_k - N_J)}$ is calculated from the singular value decomposition (SVD) of $\mathbf{R}_{\mathrm{J}_k}^{\mathrm{s}}$ [7],

$$\mathbf{R}_{\mathrm{J}_k}^{\mathrm{s}} = [\mathbf{U}_{\mathrm{s}}^{\mathrm{s}}\ \mathbf{U}_{\mathrm{n}}^{\mathrm{s}}] \begin{bmatrix} \mathbf{\Lambda}_{\mathrm{s}}^{\mathrm{s}} & \mathbf{0} \\ \mathbf{0} & \mathbf{\Lambda}_{\mathrm{n}}^{\mathrm{s}} \end{bmatrix} \begin{bmatrix} (\mathbf{U}_{\mathrm{s}}^{\mathrm{s}})^H \\ (\mathbf{U}_{\mathrm{n}}^{\mathrm{s}})^H \end{bmatrix}. \tag{6}$$

B. Impact of Time-varying Correlation

Theorem 1: Let

$$\mathbf{\Sigma}_{\mathrm{J}}^{\mathrm{s}} = \mathbf{V}^{\mathrm{s}} \mathbf{S}^{\mathrm{s}} (\mathbf{V}^{\mathrm{s}})^H \text{ and } \mathbf{\Sigma}_{\mathrm{J}}^{\mathrm{d}} = \mathbf{V}^{\mathrm{d}} \mathbf{S}^{\mathrm{d}} (\mathbf{V}^{\mathrm{d}})^H$$

be the SVD of $\mathbf{\Sigma}_{\mathrm{J}}^{\mathrm{s}}$ and $\mathbf{\Sigma}_{\mathrm{J}}^{\mathrm{d}}$, where $\mathbf{\Sigma}_{\mathrm{J}}^{\mathrm{s}}$ and $\mathbf{\Sigma}_{\mathrm{J}}^{\mathrm{d}}$ are the values of $\mathbf{\Sigma}_{\mathrm{J}}$ in the silent period and data transmission period, respectively. Let $\mathbf{F}$ be the "virtual change" factor given by

$$\mathbf{F} = \mathbf{V}^{\mathrm{d}} \sqrt{\mathbf{S}^{\mathrm{d}} (\mathbf{S}^{\mathrm{s}})^{-1}} (\mathbf{V}^{\mathrm{s}})^H. \tag{7}$$

Then, the change over time from $\mathbf{\Sigma}_{\mathrm{J}}^{\mathrm{s}}$ to $\mathbf{\Sigma}_{\mathrm{J}}^{\mathrm{d}}$ causes a "virtual change" in the jamming channel from $\mathbf{Z}_k$ to $(\mathbf{Z}_k \mathbf{F})$.

Proof: The proof is given in Appendix A. ■

Note that $\mathbf{\Sigma}_{\mathrm{J}}^{\mathrm{s}}$ can be expressed by

$$\mathbf{\Sigma}_{\mathrm{J}}^{\mathrm{s}} = \begin{bmatrix} \sigma_1^2 & \rho_{12}^{\mathrm{s}} \sigma_1 \sigma_2 & \dots & \rho_{1J}^{\mathrm{s}} \sigma_1 \sigma_{N_J} \\ (\rho_{12}^{\mathrm{s}})^* \sigma_1 \sigma_2 & \sigma_2^2 & \dots & \rho_{2J}^{\mathrm{s}} \sigma_2 \sigma_{N_J} \\ \dots & \dots & \dots & \dots \\ (\rho_{1J}^{\mathrm{s}})^* \sigma_1 \sigma_{N_J} & (\rho_{2J}^{\mathrm{s}})^* \sigma_2 \sigma_{N_J} & \dots & \sigma_{N_J}^2 \end{bmatrix}, \tag{8}$$

where σ_j^2 is the variance of the jth transmitted jamming signal, and ρ_{ij}^{s} is the complex correlations coefficient between the ith and jth transmitted jamming signals in the inter-frame silent period, with $i, j \in \{1, 2, ...N_J\}$. The complex correlations coefficient ρ_{ij}^{s} can be calculated as [15, p. 87]

$$\rho_{ij}^{\mathrm{s}} = \frac{\mathbb{E}(\mathbf{X}_{\mathrm{J}i}^{\mathrm{s}} (\mathbf{X}_{\mathrm{J}j}^{\mathrm{s}})^H)}{\sigma_i \sigma_j}. \tag{9}$$

Examining the behavior of $\mathbf{F}$ provides us interesting insights about the impact of the change in the correlations between transmitted jamming signals on the "virtual change" in the jamming channel. The first observation is for the case of unchanged (i.e., over each frame) correlations. In this case, $\mathbf{\Sigma}_{\mathrm{J}}^{\mathrm{d}} = \mathbf{\Sigma}_{\mathrm{J}}^{\mathrm{s}}$, $\mathbf{V}^{\mathrm{d}} = \mathbf{V}^{\mathrm{s}}, \mathbf{S}^{\mathrm{d}} = \mathbf{S}^{\mathrm{s}}$, and $\mathbf{F} = \mathbf{I}$. Therefore, $(\mathbf{Z}_k \mathbf{F}) = \mathbf{Z}_k$, and there is no "virtual change" in the jamming channel. The second observation is for the case of time-varying correlations, and is described by the following corollary.

Corollary 1.1: When $\mathbf{\Sigma}_{\mathrm{J}}^{\mathrm{d}} \neq \mathbf{\Sigma}_{\mathrm{J}}^{\mathrm{s}}$ and $|\rho_{ij}^{\mathrm{s}}| \to 1$ for $i \neq j$, the elements of the "virtual change" factor $\mathbf{F}$ approach infinity, results in a significant "virtual change" in the jamming channel.

Proof: The proof is given in Appendix B. ■

Therefore, there is a "virtual change" in the jamming channel observed by the receiver when the correlations between transmitted jamming signals vary over time. The "virtual change" is significant when $|\rho_{ij}^{\mathrm{s}}| \to 1$ for $i \neq j$. It implies that, from the receiver's observation, the estimated left nullspace becomes ineffective when the correlations is high and largely changed. Therefore, using $\hat{\mathbf{Q}}_k^{\mathrm{s}}$ to generate $\mathbf{W}_k$ may not guarantee jamming nullification in the data

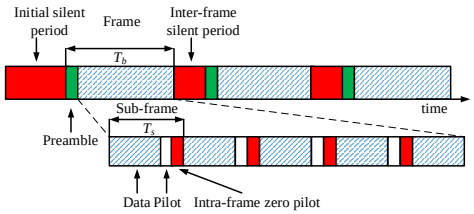

Fig. 2: Protocol for the case with time-varying correlations.

transmission period. The case of time-varying correlations between transmitted jamming signals will be considered in more detail in Subsection IV-B.

IV. Interference Nullification with Correlated Transmitted Interference Signals

A. Unchanged Non-zero Correlation

This subsection considers the case with $T_\rho \geq T_b$, where T_ρ denotes the correlation coherence time, over which the change in the correlations is negligible, and T_b is the time interval of one frame as illustrated in Fig. 1. As described in the first observation on the behavior of $\mathbf{F}$, when the correlations is constant over time, there is no "virtual change" in the jamming channel. As a result, the beam-forming matrix $\mathbf{W}_k$, which is derived from $\hat{\mathbf{Q}}_k^{\mathrm{s}}$, can be used to nullify $\mathbf{y}_{\mathrm{J}_k}^{\mathrm{d}}$, regardless of the value of the correlations between transmitted jamming signals.

Therefore, jamming signals with non-zero and unchanged correlations can be suppressed in the same manner as the uncorrelated jamming signals. In these cases, we only have to handle the time-varying channels, but not the time-varying correlations. Hence, the protocol in Fig. 1 can be used to nullify the jamming signals and perform BS-UE communication.

B. Varying Non-zero Correlation

This subsection considers the case of $T_\rho < T_b$, meaning the correlations between transmitted jamming signals vary rapidly enough, such that during the frame interval T_b, the change in the correlations is not negligible. As stated in Theorem 1, the change in the correlations causes a "virtual change" in the jamming channel, characterized by the "virtual change" factor $\mathbf{F}$. From Corollary 1.1, when $\mathbf{\Sigma}_{\mathrm{J}}^{\mathrm{d}} \neq \mathbf{\Sigma}_{\mathrm{J}}^{\mathrm{s}}$ and one or more $|\rho_{ij}^{\mathrm{s}}|$ approach 1, there is a significant "virtual change" in the jamming channel, make it unable to use $\mathbf{W}_k$, which derived from $\hat{\mathbf{Q}}_k^{\mathrm{s}}$, to nullify $\mathbf{y}_{\mathrm{J}_k}^{\mathrm{d}}$.

A potential solution to the change in the correlations is to decrease the frame time interval to $T_b \leq T_\rho$. However, more frequent tracking of $\hat{\mathbf{Q}}_k^{\mathrm{s}}$ means less BS-UE data transmission time. A suitable value of T_b should be based on two factors: the jamming channel's coherence time T_c and the correlation coherence time T_ρ. For example, the longer T_c or T_ρ, the longer T_b should be. While the first factor depends on the nature of the jamming channel environment, and its value can be predicted based on field measurement, we cannot control or predict the second factor.

Given the above, we develop a communication protocol capable of dealing with the change of the correlations between transmitted jamming signals, as shown in Fig. 2 and Algorithm 1. Each frame in Fig. 2 is divided into N_{sf} sub-frames, each of

Algorithm 1 Protocol for time-varying correlations and time-varying channels.

1: Acquire or update $\hat{\mathbf{Q}}_k^{\mathrm{s}}$ during silent periods.
2: Design $\mathbf{W}_k$ from $\hat{\mathbf{Q}}_k^{\mathrm{s}}$.
3: Estimate $\mathbf{H}_k^{\mathrm{eq}}$, calculate $\mathbf{G}_k$.
4: Perform BS-UE data transmission.
5: $n_{\mathrm{sf}} \leftarrow 1$
6: **while** $n_{\mathrm{sf}} \leq N_{\mathrm{sf}} - 1$ **do**
7: Update $\mathbf{G}_k$ using $\mathbf{x}_{\mathrm{m}_k}$.
8: Measure $\gamma_{\mathrm{J}} = ||\mathbf{r}_k||^2/||\mathbf{p}_k||^2$ using $\mathbf{x}_{\mathrm{m}_k}$.
9: **if** $\gamma_{\mathrm{J}} \geq \gamma_{\mathrm{r}}$ **then**
10: Start intra-frame zero pilot.
11: Estimate $\mathbf{Q}_k^{\mathrm{J}}$ during intra-frame zero pilot.
12: Design $\mathbf{W}_k^{\mathrm{i}}$ from $\hat{\mathbf{Q}}_k^{\mathrm{J}}$.
13: Update equivalent channel $\mathbf{H}_k^{\mathrm{eq}} \leftarrow \mathbf{W}_k^{\mathrm{i}}\mathbf{W}_k^H\mathbf{H}_k^{\mathrm{eq}}$.
14: Update beam-forming matrix $\mathbf{W}_k \leftarrow \mathbf{W}_k^{\mathrm{i}}$.
15: **end if**
16: Perform BS-UE data transmission.
17: $n_{\mathrm{sf}} \leftarrow n_{\mathrm{sf}} + 1$
18: **end while**
19: Repeat from step 1.

length $T_s = T_b/N_{\mathrm{sf}}$. Each sub-frame consists of data payload and pilot samples $\mathbf{x}_{\mathrm{m}_k}$, which is used to measure the jamming residual. When the measured jamming residual is higher than a predefined value, intra-frame zero pilot is used to update the beam-forming matrix $\mathbf{W}_k$, as described below.

By using the pilot signal $\mathbf{x}_{\mathrm{m}_k}$, the jamming residual can be measured by

$$\mathbf{r}_k = \mathbf{p}_k - \mathbf{W}_k(\mathbf{H}_k\mathbf{P}_k\mathbf{x}_{\mathrm{m}_k} + \mathbf{H}_k\sum_{l\neq k}^{K}\mathbf{P}_l\mathbf{x}_l) = \mathbf{W}_k(\mathbf{Z}_k\mathbf{x}_{\mathrm{J}} + \mathbf{n}).$$

When $\gamma_{\mathrm{J}} = ||\mathbf{r}_k||^2/||\mathbf{p}_k||^2$ exceeds a pre-defined threshold γ_{r}, the BS starts sending intra-frame zero pilots, and $\mathbf{Q}_k^{\mathrm{J}}$ is estimated using the SVD as described in Section III. Note that $\mathbf{Q}_k^{\mathrm{J}}$ denotes a matrix whose rows form an orthornomal basis for the left nullspace of the received signal at the kth UE in the intra-frame silent period. The new beam-forming matrix $\mathbf{W}_k^{\mathrm{i}}$ is obtained from $\hat{\mathbf{Q}}_k^{\mathrm{J}}$, which is the estimated value of $\mathbf{Q}_k^{\mathrm{J}}$.

To reduce the overhead, the equivalent channel is only estimated using training signal and an MMSE or LS estimator once per frame. For each sub-frame, when intra-frame zero pilot is used, $\mathbf{H}_k^{\mathrm{eq}}$ is replaced by $\mathbf{H}_k^{\mathrm{eq\_in}}$ given by

$$\mathbf{H}_k^{\mathrm{eq\_in}} = \mathbf{W}_k^{\mathrm{i}}\mathbf{H}_k\mathbf{P}_k = \mathbf{W}_k^{\mathrm{i}}\mathbf{W}_k^H\mathbf{W}_k\mathbf{H}_k\mathbf{P}_k = \mathbf{W}_k^{\mathrm{i}}\mathbf{W}_k^H\mathbf{H}_k^{\mathrm{eq}}.$$

By using the pilots signal $\mathbf{x}_{\mathrm{m}_k}$ and intra-frame zero pilots, we divide each frame with a time interval T_b into N_{sf} sub-frames with a time interval T_s. This division significantly reduces the change in the correlations between transmitted jamming signals and reduces the elements of the "virtual change" factor $\mathbf{F}$. Therefore, jamming nullification performance can be significantly improved.

It is worth noting that we can start an inter-frame silent period as soon as γ_{J} exceeds γ_{r}. However, starting a new inter-frame silent period requires the BS-UE synchronization and $\mathbf{H}_k^{\mathrm{eq}}$ estimation to be performed again. Therefore, BS-UE communication time is reduced dramatically when T_ρ decreases. Therefore, using the intra-frame zero pilot is a more suitable approach to reduce the system's overhead and increase

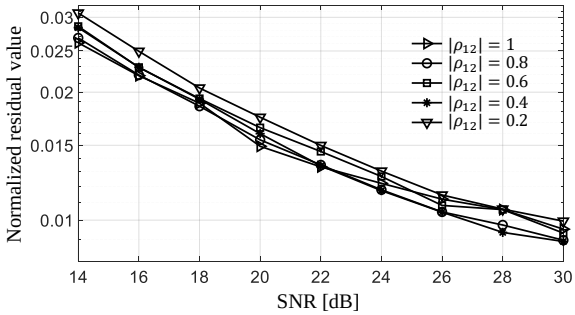

Fig. 3: r_{J} values when $|\rho_{12}|$ is unchanged.

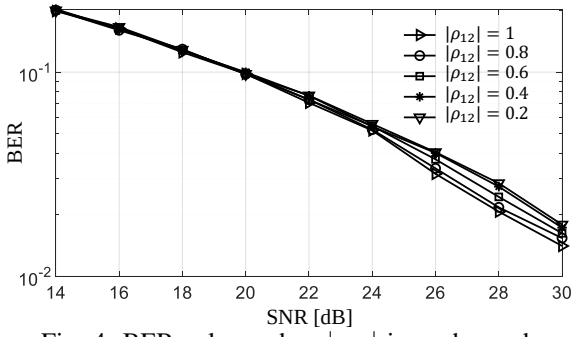

Fig. 4: BER values when $|\rho_{12}|$ is unchanged.

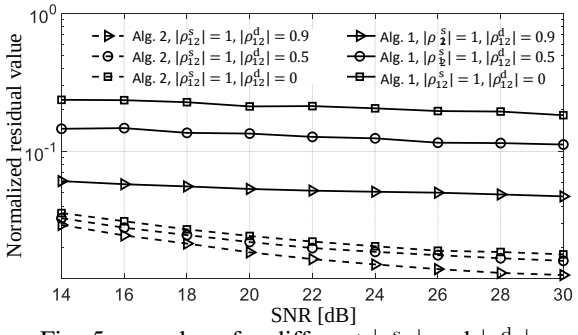

Fig. 5: r_{J} values for different $|\rho^{\mathrm{s}}_{12}|$ and $|\rho^{\mathrm{d}}_{12}|$.

BS-UE communication time.

V. Simulation results

This section presents the simulation results to validate our proposed schemes. The performance metrics include the normalized residual value $r_{\mathrm{J}} = \frac{||\hat{\mathbf{Q}}^{\mathrm{s}}_k \mathbf{y}^{\mathrm{d}}_{\mathrm{J}_k}||^2}{||\mathbf{y}^{\mathrm{d}}_{\mathrm{J}_k}||^2}$ and the bit error rate (BER). The simulation parameters are as follows unless otherwise stated. A single carrier narrowband MIMO system is considered with a bandwidth of 200 kHz and a center frequency of 447 MHz. We use 16 Quadrature Amplitude Modulation (QAM) with no forward error correction (FEC) coding. Both BS-UE and jammers-UE channels are modeled using a flat fast fading Rician model from [12] with a Doppler frequency of $F_d = 24.83$ Hz (i.e., corresponding to BS-UE and jammers-UE relative speeds of about 60 km/h), a Rician factor of 5 and the number of propagation paths for each signal is 5. The BS and UE are assumed to have a uniform linear array (ULA) of 12 and 8 antennas, respectively. The BS is communicating with $K = 4$ UEs, and the number of data streams for each user is $D_k = 4$. The number of samples for each frame, each initial silent period, each inter-frame zero pilot, each intra-frame zero pilot, and each $\mathbf{x}_{\mathrm{m}_k}$ are 240, 64, 5, 5 and 5, respectively. All the simulation results are obtained by averaging over 500 independent trials.

A. Unchanged Non-Zero Correlations

In this sub-section, we present the simulation results for the case of non-zero correlations between transmitted jamming signals, and with $T_\rho \geq T_b$, such that the correlations are considered constant over each frame. As discussed in Subsection IV-A, when the correlations between the transmitted jamming signals are non-zero and constant, there is no "virtual change" in the jamming channel. As a result, we only have to deal with time-varying physical channels. Therefore, the protocol in Fig. 1 can be used to nullify jamming signals and perform BS-UE communication.

Fig. 3 illustrates r_{J} values as a function of the jamming signal's SNR for different values of $|\rho^{\mathrm{s}}_{12}| = |\rho^{\mathrm{d}}_{12}| = |\rho_{12}|$. As can be seen, r_{J} has similar values for different $|\rho_{12}|$ values, meaning $|\rho_{12}|$ value have a little impact on the jamming nullification performance. As a result, the system achieves similar BER performance for different values of $|\rho_{12}|$, as illustrated in Fig. 4.

B. Time-varying Correlations

In this sub-section, we present the simulation result for the case of time-varying correlations with $T_\rho < T_b$. As discussed in Subsection IV-B, in this case we have to deal with both time-varying channel and "virtual change" in the jamming channel due to the time-varying correlations between transmitted jamming signals. To deal with those issues, we use the protocol illustrated in Fig. 2 and Algorithm 1 with $N_{\mathrm{sf}} = 5$ and $\gamma_{\mathrm{r}} = 0.05$. Note that in this simulation, the correlations between transmitted jamming signals are assumed to change linearly. Therefore, the changes from $|\rho^{\mathrm{s}}_{12}|$ into $|\rho^{\mathrm{d}}_{12}|$ over one frame is equally divided into $N_{\mathrm{sf}} = 5$ changes over each sub-frame.

Fig. 5 illustrates the values of r_{J} for different scenarios of the time-varying correlations between transmitted jamming signals. As can be seen, there are large jamming residual values for the system using the protocol in Fig. 1. It means the protocol in Fig. 1 is unable to catch the "virtual change" in the jamming channel, caused by the change in the correlations between transmitted jamming signals. Another phenomenon is that the jamming residual becomes larger with the larger difference between $|\rho^{\mathrm{s}}_{12}|$ and $|\rho^{\mathrm{d}}_{12}|$. That is because a larger difference between $|\rho^{\mathrm{s}}_{12}|$ and $|\rho^{\mathrm{d}}_{12}|$ results in larger elements of the "virtual change" factor $\mathbf{F}$. On the other hand, the system using the protocol in Fig. 2 and Algorithm 1 has successfully caught up the "virtual change" in the jamming channel, results in a much smaller jamming residual.

Fig. 6 compares the BER performance of the system using the protocol in Fig. 1 to that of the protocol in Algorithm 1 and Fig. 2 for different scenarios of the time-varying correlations mentioned above. As can be seen, the system using the protocol in Fig. 1 has high BER values, because

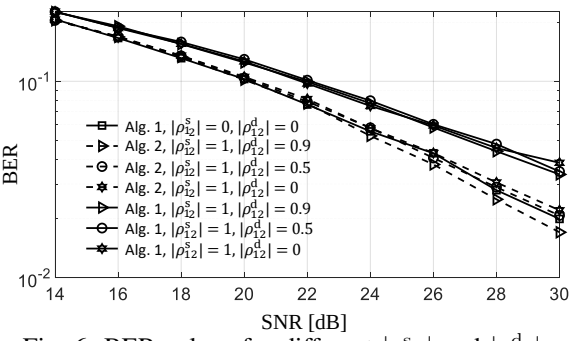

Fig. 6: BER values for different $|\rho^{\mathrm{s}}_{12}|$ and $|\rho^{\mathrm{d}}_{12}|$.

the jamming signals are not effectively nullified. On the other hand, the system using the protocol in Algorithm 1 and Fig. 2 successfully nullify the jamming signals, result in BER results similar to that of the system using the protocol in Fig. 1 for the case of uncorrelated jamming signals.

VI. Conclusion

We investigated the impact of non-zero and time-varying jamming signals' correlations on the jamming channel's nullspace estimation and jamming signals nullification. We proposed the technique to effectively suppress the jamming signals for different schemes of non-zero and varying jamming signals' correlations. Monte Carlo simulation results show that our techniques can nullify the interfering signals for different values of the correlations.

Appendix A
Proof of Theorem 1

Because the sample covariance matrix of the received jamming signal is used to estimate $\mathbf{Q}^{\mathrm{s}}_{k}$, we examine the change from $\mathbf{R}^{\mathrm{s}}_{\mathrm{J}_k}$ to $\mathbf{R}^{\mathrm{d}}_{\mathrm{J}_k}$ due to the change from $\mathbf{\Sigma}^{\mathrm{s}}_{\mathrm{J}}$ to $\mathbf{\Sigma}^{\mathrm{d}}_{\mathrm{J}}$. We assume the numbers of signal samples are sufficiently large such that the law of large number is applicable. Therefore, $\mathbf{R}^{\mathrm{s}}_{\mathrm{J}_k}$ and $\mathbf{R}^{\mathrm{d}}_{\mathrm{J}_k}$ converge to $(\mathbf{Z}_k\mathbf{\Sigma}^{\mathrm{s}}_{\mathrm{J}}\mathbf{Z}^{H}_{k} + \sigma^2_n\mathbf{I}_{N_k})$ and $(\mathbf{Z}_k\mathbf{\Sigma}^{\mathrm{d}}_{\mathrm{J}}\mathbf{Z}^{H}_{k} + \sigma^2_n\mathbf{I}_{N_k})$, respectively. Note that $\mathbf{S}^{\mathrm{s}}$ and $\mathbf{S}^{\mathrm{d}}$ are diagonal matrices, while $\mathbf{V}^{\mathrm{s}}$ is an orthogonal matrix, such that $(\mathbf{V}^{\mathrm{s}})^{H}\mathbf{V}^{\mathrm{s}} = \mathbf{I}$, we have,

$$
\begin{aligned}
&\mathbf{Z}_k\mathbf{\Sigma}^{\mathrm{d}}_{\mathrm{J}}\mathbf{Z}^{H}_{k} + \sigma^2_n\mathbf{I}_{N_k} \\
&= \mathbf{Z}_k\mathbf{V}^{\mathrm{d}}\mathbf{S}^{\mathrm{d}}(\mathbf{V}^{\mathrm{d}})^{H}\mathbf{Z}^{H}_{k} + \sigma^2_n\mathbf{I}_{N_k} \\
&= \mathbf{Z}_k\mathbf{V}^{\mathrm{d}}\sqrt{\mathbf{S}^{\mathrm{d}}(\mathbf{S}^{\mathrm{s}})^{-1}}\mathbf{S}^{\mathrm{s}}\sqrt{\mathbf{S}^{\mathrm{d}}(\mathbf{S}^{\mathrm{s}})^{-1}}(\mathbf{V}^{\mathrm{d}})^{H}\mathbf{Z}^{H}_{k} + \sigma^2_n\mathbf{I}_{N_k} \\
&= \mathbf{Z}_k\mathbf{V}^{\mathrm{d}}\sqrt{\mathbf{S}^{\mathrm{d}}(\mathbf{S}^{\mathrm{s}})^{-1}}(\mathbf{V}^{\mathrm{s}})^{H}\mathbf{V}^{\mathrm{s}}\mathbf{S}^{\mathrm{s}}(\mathbf{V}^{\mathrm{s}})^{H}\mathbf{V}^{\mathrm{s}}\sqrt{\mathbf{S}^{\mathrm{d}}(\mathbf{S}^{\mathrm{s}})^{-1}}(\mathbf{V}^{\mathrm{d}})^{H}\mathbf{Z}^{H}_{k} \\
&\quad + \sigma^2_n\mathbf{I}_{N_k} \\
&= (\mathbf{Z}_k\mathbf{F})\mathbf{V}^{\mathrm{s}}\mathbf{S}^{\mathrm{s}}(\mathbf{V}^{\mathrm{s}})^{H}(\mathbf{Z}_k\mathbf{F})^{H} + \sigma^2_n\mathbf{I}_{N_k} \\
&= (\mathbf{Z}_k\mathbf{F})\mathbf{\Sigma}^{\mathrm{s}}_{\mathrm{J}}(\mathbf{Z}_k\mathbf{F})^{H} + \sigma^2_n\mathbf{I}_{N_k}.
\end{aligned}
$$

Appendix B
Proof of Corollary 1.1

When $|\rho^{\mathrm{s}}_{ij}| \to 1$, from (8), $\mathbf{\Sigma}^{\mathrm{s}}_{\mathrm{J}}$ becomes a singular matrix. Therefore, there is one diagonal element $s^{\mathrm{s}}_{jj} \in \mathbf{S}^{\mathrm{s}}$ approaches 0 [16, p. 261]. From (7), when $s^{\mathrm{s}}_{jj} \in \mathbf{S}^{\mathrm{s}}$ approach 0 while $s^{\mathrm{d}}_{jj} \neq s^{\mathrm{s}}_{jj}$, the elements of $\mathbf{F}$ approach infinity.

Therefore, the change from $\mathbf{\Sigma}^{\mathrm{s}}_{\mathrm{J}}$ to $\mathbf{\Sigma}^{\mathrm{d}}_{\mathrm{J}}$ cause a "virtual change" in the jamming channel from $\mathbf{Z}_k$ to $(\mathbf{Z}_k\mathbf{F})$.

References

[1] K. Grover, A. Lim, and Q. Yang, "Jamming and anti-jamming techniques in wireless networks: a survey," *Int. J. Ad Hoc Ubiquitous Comput.*, vol. 17, no. 4, pp. 197–215, 2014.

[2] A. J. Fenn, *Adaptive antennas and phased arrays for radar and communications*, Boston, MA, USA, 2007.

[3] T. T. Do, E. Björnson, E. G. Larsson, and S. M. Razavizadeh, "Jamming-resistant receivers for the massive MIMO uplink," *IEEE Trans. Inf. Forensics Security*, vol. 13, no. 1, pp. 210–223, 2017.

[4] H. Akhlaghpasand, E. Björnson, and S. M. Razavizadeh, "Jamming suppression in massive MIMO systems," *IEEE Trans. Circuits Syst. II, Exp. Briefs*, vol. 67, no. 1, pp. 182–186, 2019.

[5] ——, "Jamming-robust uplink transmission for spatially correlated massive MIMO systems," *IEEE Trans. Commun.*, vol. 68, no. 6, pp. 3495–3504, 2020.

[6] Q. Yan, H. Zeng, T. Jiang, M. Li, W. Lou, and Y. T. Hou, "Jamming resilient communication using MIMO interference cancellation," *IEEE Trans. Inf. Forensics Security*, vol. 11, no. 7, pp. 1486–1499, 2016.

[7] X. G. Doukopoulos and G. V. Moustakides, "Fast and stable subspace tracking," *IEEE Trans. Signal Process.*, vol. 56, no. 4, pp. 1452–1465, 2008.

[8] Y. Léost, M. Abdi, R. Richter, and M. Jeschke, "Interference rejection combining in LTE networks," *Bell Labs Tech. J.*, vol. 17, no. 1, pp. 25–49, 2012.

[9] M. H. Brady, M. Mohseni, and J. M. Cioffi, "Spatially-correlated jamming in gaussian multiple access and broadcast channels," in *Proc. CISS*, Princeton, NY, USA, Mar. 2006, pp. 1635–1639.

[10] J. Gao, S. A. Vorobyov, H. Jiang, and H. V. Poor, "Worst-case jamming on MIMO Gaussian channels," *IEEE Trans. Signal Process.*, vol. 63, no. 21, pp. 5821–5836, 2015.

[11] T.-J. Shan, M. Wax, and T. Kailath, "On spatial smoothing for direction-of-arrival estimation of coherent signals," *IEEE Trans. Acoust., Speech, Signal Process.*, vol. 33, no. 4, pp. 806–811, 1985.

[12] C. Xiao, Y. R. Zheng, and N. C. Beaulieu, "Novel sum-of-sinusoids simulation models for Rayleigh and Rician fading channels," *IEEE Trans. Wireless Commun.*, vol. 5, no. 12, pp. 3667–3679, 2006.

[13] G. Strang, *Introduction to linear algebra*. Wellesley, MA, USA: Wellesley-Cambridge Press, 2016.

[14] A. Kekirigoda, K.-P. Hui, Q. Cheng, Z. Lin, A. Zhang, J. Zhang, D. Nguyen, and X. Huang, "Massive MIMO for tactical ad-hoc networks in RF contested environments," in *IEEE/AFCEA Mil. Commun. Conf. (MILCOM)*, 2019.

[15] P. J. Schreier and L. L. Scharf, *Statistical signal processing of complex-valued data: the theory of improper and noncircular signals*. Cambridge, UK: Cambridge Univ. Press, 2010.

[16] G. H. Golub and C. F. Van Loan, *Computation Matrix*. Baltimore, MD: Johns Hopkins Univ. Press, 2013.